Multiband Gravitational-Wave Astronomy: Detectors, Source Populations, and Precision Tests

Meenu Mohil[1*], Vijay Rawat[2]

[1]Associate Professor, Department of Physics, Acharya Narendra Dev College, University of Delhi, Delhi 110019, India
Corresponding Author Email: *mohil.meenu[at]gmail.com*

[2]Student, Department of Physics, Acharya Narendra Dev College, University of Delhi, Delhi 110019, India

Abstract: ***Albert Einstein first proposed the existence of gravitational waves in 1916 as a consequence of his general Theory of Relativity. For nearly a century, these waves remained purely theoretical until 2015, when the Laser Interferometer Gravitational-Wave Observatory (LIGO) and Virgo detectors achieved the first direct detection of a binary black hole merger. This breakthrough marked the beginning of gravitational-wave astronomy, now supported by the KAGRA detector, forming the LIGO-Virgo-Kagra (LVK) collaboration. Since then, more than ninety compact binary coalescences have been confirmed. During the ongoing fourth observing run (O4, 2023-2025), over two hundred public alerts have already been issued, including 128 new confirmed candidates in the GWTC-4.0 catalogue. These results are made possible by improved detector sensitivity, reduced quantum noise, and advances in data analysis methods such as matched filtering, machine learning algorithms, convolutional neural networks, and normalizing flows. This review outlines the theoretical background, observational developments, and data analysis framework of gravitational-wave science in a way that supports both undergraduate and postgraduate teaching in relativity and astrophysics. It discusses how detectors- from ground-based interferometers like LIGO, Virgo and KAGRA, to pulsar timing arrays (such as NANOGrav and EPTA) and space missions like LISA-cover a wide frequency range, from nanohertz to kilohertz. The paper also traces the transition from isolated detection to large-scale population studies through the successive observing runs. The review includes a case study of orbital parameter estimation that provides examples to be used in classroom simulations using open-access data. The wider themes associated with these ideas include multi-messenger astronomy, cosmological distance measurements, and gravitational physics precision tests. Easy access to open data sources such as GWOSC gives instructors the opportunity to teach students about the waveform analysis and statistical inference processes in a very practical manner.***

Keywords: Gravitational waves, general relativity, matched filtering, compact binary coalescences, multi-messenger astronomy

1. Introduction

In general theory of relativity, Einstein offers a formulation of spacetime that is no longer a static space, but a dynamic elastic geometry that gets distorted by the occurrence of mass and energy. These oscillations are known as gravitational waves (GWs), and they are emitted when massive and compact objects such as black holes or neutron stars accelerate. During the period of 1916-1918, Einstein showed that transverse disturbance could be generated by these accelerations with a speed of light and it can transport energy through space by providing the approximate solutions of his own field equations. General relativity This theory, based on his formulation of the general relativity idea of gravity in 1915, supersedes the Newtonian concept of gravity as the mass-energy distribution of the spacetime curvature. As much as the mathematical foundation of the theory was persuasive, the initial physicists doubted that GWs were real entities or were just an artifact of coordinates (Abbott et al. 2016). This perception changed with subsequent research, in particular with the formula of quadrupole radiations, had shown that these waves remove energy out of the emitting system (Bishop & Rezzolla 2016). This discovery made gravitational-wave astronomy an open door to the astrophysical environment frontiers. In the case of teaching relativity at the university level, this is a good introduction to relativity. Starting with a simple example of how distortions of spacetime can change a movement, students can imagine how waves propagate with the help of these distortions. This theoretical model is based on t equation (1) formulated by Einstein in 1915 and developed in 1916 which show the relationship between the curvature of spacetime and the energy-momentum trapped in the spacetime:

$$G_{\mu\nu} = \frac{8\pi G}{c^4} T_{\mu\nu} \quad (1)$$

Here, the Einstein tensor $G_{\mu\nu} = R_{\mu\nu} - \frac{1}{2} R g_{\mu\nu}$ combines the Ricci tensor $R_{\mu\nu}$, scalar curvature R, and the metric tensor $g_{\mu\nu}$. The stress-energy tensor $T_{\mu\nu}$ represents the density and flux of energy and momentum, while G and c denote the gravitational constant and the speed of light, respectively. Conceptually, concentrations of mass and energy curve spacetime, guiding the motion of nearby objects.

In the weak-field limit, where gravitational effects are small and far from massive sources, the metric can be expressed as a small perturbation of flat spacetime, $g_{\mu\nu} = \eta_{\mu\nu} + h_{\mu\nu}$, with $, |\, h_{\mu\nu} \,| \ll 1$. In the transverse-traceless (TT) gauge, these perturbations propagate at light speed as waves with two orthogonal polarization states plus (+) and cross (×) that alternately stretch and compress test masses, the effect measured by LIGO (Aasi et al. 2015) as shown in equation (2). Online tools and demonstrations using simple test-mass models help students visualize this polarization behaviour effectively. Einstein's 1918 derivation of the quadrupole formula provided the fundamental expression for GW emission in weak fields:

$$h_{ij}^{\mathrm{TT}}(t, \mathrm{r}) = \frac{2G}{c^4 r} \ddot{I}_{ij}^{\mathrm{TT}}\left(t - \frac{r}{c}\right), \quad (2)$$

Where r is the distance from the source, and $\ddot{I}_{ij}^{TT}$ the second time-derivative of the traceless quadrupole moment (Bishop & Rezzolla 2016). The corresponding energy flux is given by equation (3)

$$\left\langle \frac{dE}{dt} \right\rangle = -\frac{G}{5c^5} \Sigma_{ij} \left(\frac{d^3 I_{ij}}{dt^3}\right)^2, \quad (3)$$

Which shows that radiation arises only from time-varying, asymmetries mass distributions such as eccentric binary systems. Later studies removed the question of coordinate dependence, and made GWs accepted carriers of energy. As the development of the theory continued, the experimental proof required decades. The earliest indirect evidence was provided in 1974 with the publication of the Hulse-Taylor binary pulsar PSRB13+16 whose orbital decay predicted with GW energy loss with precise accuracy (Weisberg & Huang 2016). By 2005 the rate of orbital contraction observed was consistent with theoretical models to within 0.2% and was awarded the 1993 Nobel Prize in Physics. This achievement bridged the gap between the theoretical predictions and observational evidence.

Direct detection, however, required engineering capable of measuring strains as small as $h \approx 10^{-21}$ from distant sources. Joseph Weber's resonant bar detectors in the 1960s represented the earliest attempts but lacked sufficient sensitivity (Abbott et al. 2023). Subsequent improvements, including cryogenic techniques and prototype interferometers, laid the ground work for modern laser interferometric detectors. The breakthrough came on 14 September 2015, when the Advanced LIGO detectors observed GW150914 —a binary black hole merger involving 36 M_{Θ} and 29 M_{Θ} components at a distance of about 410Mpc—with a waveform consistent with predictions of general relativity. This detection not only confirmed the existence of stellar-mass black holes about also inaugurated the era of gravitational-wave astronomy. The later observing runs broadened the initial discovery set (Abbott et al. 2023). O2 (2016–2017) and O3 (2019–2020) detected many more black-hole mergers and several neutron-star events, including the landmark GW170817, which was observed alongside gamma rays, a kilonova, and an afterglow signal (Abbott et al. 2017). These runs also revealed systems with unexpected spins and masses in gap regions (Abbott et al. 2021; Abbott et al. 2017). GW170817 proved especially influential, providing a new standard-siren estimate of the Hubble constant and confirming r-process heavy-element production.

The O3 observing campaign yielded more than ninety confirmed gravitational-wave signals, providing the basis for detailed studies of binary-compact-object populations and several tests of general relativity. The ongoing O4 run (2023–2025), divided into O4a and O4b, has already surpassed 128 detections in its first phase, reflecting major upgrades such as improved quantum squeezing, seismic isolation, and calibration. These enhancements are expected to push total detections beyond 200, allowing more precise studies of compact binaries and cosmology. In parallel, waveform models now include spin precession, higher modes, and eccentricity, while modern analysis pipelines increasingly use Bayesian methods and machine-learning tools—such as CNNs and normalizing flows—to accelerate event identification and parameter estimation with high accuracy (Abbott et al. 2019).

In general, the study of gravitational-wave astronomy has developed since being a theorical assumption to a fully developed field that incorporates experimental, computational, and educational aspects. Its advancements provide courses of linking theoretical underpinnings, numerical and multi-messenger observations throughout the undergraduates and postgraduate course. The main points of discussion in this review are: (i) developments in the process of the O4 run (Chen & Hido 2025; Sun et al. 2023); (ii) developments in the waveform modelling and analysis, in the area of orbital eccentricity, in particular (Chatziioannou et al. 2017; Liu et al. 2024); (iii) prospects of multi-band and multi-messenger studies between ground-based detectors, pulsar timing arrays and future space missions such as LISA (Abbott et al. 2017; Armano et al. 2003). All these developments are leading towards gravitational-wave science, from its conceptual beginnings to the current frontier of precision sc (Abbott et al. 2016; Will 2014).

2. Theoretical Background

Space-time in general relativity can be visualised as a continuous and elastic geometry that distorts in response to mass and energy. Gravitational waves (GWs) appear as minute oscillations or ripples within this geometry when massive bodies accelerate, disturbing the surrounding curvature. This concept lies at the core of Einstein's general relativity (GR), formulated in 1915, which redefines gravity not as an attractive force but as the manifestation of curved spacetime caused by energy and momentum. Massive objects, therefore, guide the motion of nearby bodies by shaping the geometry in which they move, rather than exerting any direct mechanical pull (Abbott et al. 2016; Will 2014). At the Core of GR are the Einstein field equations, which link the structure of spacetime to the matter and energy it contains:

$$G_{\mu\nu} = \frac{8\pi G}{c^4} T_{\mu\nu},$$

Where the Einstein tensor $G_{\mu\nu} = R_{\mu\nu} - \frac{1}{2} R g_{\mu\nu}$ combines the Ricci tensor $R_{\mu\nu}$, scalar curvature R, and the metric tensor $g_{\mu\nu}$. The stress-energy tensor $T_{\mu\nu}$ describes the density and flux of energy and momentum, while G is the gravitational constant and c is the speed of light. These coupled, nonlinear equations govern how spacetime curvature arises from matter and energy, and in turn, how that curvature directs the motion of particles and fields (Will 2014). In a vacuum, where $T_{\mu\nu} = 0$. The equations reduce to $R_{\mu\nu} = 0$, which admits stationary and dynamic solutions such as the Schwarzschild black hole and gravitational-wave propagation (Maggiore 2000; Schutz 1984).

Einstein's early studies between 1916 and 1918 applied linear approximations to these equations, showing that accelerating masses produce disturbances that propagate through spacetime as waves. Unlike electromagnetic radiation, gravitational waves interact extremely weakly with matter, allowing them to traverse the universe with minimal absorption or scattering and to provide direct insight into their astrophysical origins, from compact binaries to stellar explosions (Weisberg & Huang 2016). However, because of the nonlinear nature of Einstein's equations, exact analytical solutions are difficult to obtain, and approximations are typically required for practical applications (Poisson 2011). In regions where gravitational fields are weak, a linearised approach provides a useful simplification. The metric tensor can be written as a small perturbation on flat Minkowski spacetime,

$$g_{\mu\nu} = \eta_{\mu\nu} + h_{\mu\nu}, | h_{\mu\nu} | \ll 1,$$

Neglecting higher-order terms in $h_{\mu\nu}$. Applying the Lorenz gauge condition, $\partial^{\mu}\bar{h}_{\mu\nu} = 0$, where $\bar{h}_{\mu\nu} = h_{\mu\nu} - \frac{1}{2}\eta_{\mu\nu}h$, leads to the linearized wave equation,

$$\Box\bar{h}_{\mu\nu} = -\frac{16\pi G}{c^4}T_{\mu\nu},$$

With the d'Alembert operator $\Box = \partial^{\mu}\partial_{\mu}$ [Finn 1992]. In a vacuum, this simplifies to $\Box\bar{h}_{\mu\nu} = 0$, confirming that perturbations in spacetime propagate at the speed of light, analogous to waves in a massless field (Sathyaprakash & Schutz 2009). This linearised formulation effectively describes distant or weak sources such as the late inspiral phase of compact binaries, while the strong-field regime of mergers and ringdowns requires full numerical solutions to the Einstein equations [Cutler & Flanagan 1994; Baumgarte & Shapiro 2003].

For a wave travelling along the z-axis, the transverse-traceless (TT) gauge isolates the physical components of the metric perturbation, removing coordinate-dependent effects. The remaining components are expressed as:

$$h_+(t) = h_{xx} = -h_{yy}, \qquad h_\times(t) = h_{xy} = h_{yx},$$

representing the two-polarisation state of the waves—plus (+) and cross (×). The plus polarisation alternately stretches and compresses spacetime along orthogonal directions, while the cross polarization alternately stretches and compress spacetime along orthogonal directions, while the cross polarisation shears the geometry at 45° (Kidder 2008). The superposition of these two components reproduces any arbitrary GW polarisation depending on the source's inclination and orientation. Interferometers such as LIGO detect these effects by measuring relative changes in arm lengths, typically on the order of $\frac{\Delta L}{L} \approx \frac{h}{2}$. Alternative theories of gravity may predict additional scalar or vector polarisation modes, but current GW observations remain fully consistent with the tensorial predictions of GR (Yunes & Siemens 2013). Interactive simulation tools allow students to visualise these effects by observing how test masses are displaced under different modes. In the non-relativistic limit, the quadrupole term dominates the multipole expansion of GW radiation (Peters & Mathews 1963). At large distances, the TT component of the strain is given by:

$$h_{ij}^{TT}(t,r) = \frac{2G}{c^4 r}\ddot{I}_{ij}^{TT}\left(t - \frac{r}{c}\right),$$

where $\ddot{I}_{ij}^{\mathrm{TT}}$ denotes the second time derivative of the traceless quadrupole moment at a distance r. For a binary system, the asymmetric mass distribution generates a characteristic inspiral waveform (Blanchet 2014). The corresponding time-averaged energy flux is expressed as:

$$\frac{dE}{dt} = \frac{G}{5c^5}\left\langle \sum_{ij}\left(\frac{d^3 I_{ij}}{dt^3}\right)^2 \right\rangle$$

This mechanism forms the theoretical foundation for waveform templates used in matched filtering, parameter estimation, and tests of general relativity. Inclusion of higher-order multipole moments, like octupole, refines these models, thus improving the accuracy of predictions for spinning and eccentric binaries (Arun et al. 2005; Ajith et al. 2011). Spin effects further influence GW emission. The intrinsic spins of compact objects couple with the orbital angular momentum through spin-orbit and spin-spin interactions, altering both the phase evolution and amplitude of the signal. The effective aligned spin parameter establishes the change in the rate of

$$\chi_{\mathrm{eff}} = \frac{m_1\chi_{1z} + m_2\chi_{2z}}{m_1 + m_2}$$

inspiralling as compared to when no spin is considered. The in-plane spin χ p generates amplitude and phase modulations, particularly in a system with unequal masses or misaligned spins and results in precession, as well as characteristic structures of waveforms (Hannam et al. 2014). The inclusion of spin dynamics in both post-Newtonian (PN) and numerical relativity schemes is crucial to the precise inference of parameters, as well as populations, and strong-field tests of GR (Buonanno & Damour 1999). The angular emission pattern is also further enriched with additional multipole moments of the current. In an educational example, the phase shift between ten cycles at a (30+30M) Theta binary 5 of a basic exercise of the MATLAB can show the phase shift of about 10 percent, and the effects of considering these effects in the detector modelling should not be ignored. The existence of GWs as a physical reality was a decades-long dispute after being predicted by Einstein.

It was not until the mid-twentieth century that researchers such as Bondi and his collaborators provided rigorous proofs demonstrating that gravitational waves carry energy and momentum independent of coordinates choices (Bondi et al. 1959). The discovery of the Hulse-Taylor binary pulsar PSRB1913+16 in 1974 confirmed this picture, with its observed orbital decay matching quadrupole radiation predictions to high precision, a result recognized by the 1993 Noble Prize (Weisberg & Huang 2016). These early investigations form the basis of contemporary gravitational-wave searches and waveform construction techniques (Blanchet 2014).

3. Detector Networks and Observing Runs

3.1 Existing and Planned Detectors

Gravitational-wave (GW) astronomy is an international scientific project, in which a network of interferometers on the ground, space missions, and pulsar timing arrays are coordinated to investigate frequencies ranging over fifteen orders of magnitude, with nanohertz to kilohertz frequencies. These instruments, used in a coordinated manner, allow to observe the compact-object mergers, study the supermassive black holes, and explore the stochastic GW background that was created by the early universe (Sathyaprakash et al. 2012). The development of first Advanced LIGO prototypes (figure 1) to future observatories like LISA and the Einstein Telescope shows how technical advances have been continually extending the field of view of gravitational-wave science (Punturo et al. 2010). The centre of the existing detection network consists of the ground-based laser interferometers, which are played by the frequencies range of about 10Hz up to 10kHz mainly [5]. The Laser Interferometer Gravitational-Wave Observatory (LIGO) is an arrangement of two installations in Hanford, Washington, and Livingston, Louisiana, which is set to reach strain sensitivities of approximately 10 -23 Hz -1/2 (Aasi et al. 2015). In 2015, the Advanced LIGO detectors became sensitive to their design sensitivity, and the first direct gravitational wave source, GW150914, was detected. Virgo located just outside Pisa, Italy, is complementary to LIGO, and it has longer arms that enhance localisation to the source (Acernese et al. 2015). Japan's KAGRA facility is strategically constructed underground within the Kamioka mine, employing cryogenically cooled mirrors and advanced seismic isolation to further suppress environmental noise (Akutsu et al. 2021). Together, these facilities from the LIGO-Virgo-LKAGRA (LVK) collaboration, which has conducted four major observing runs, each improving in sensitivity and detection rates as detailed in Table 1.

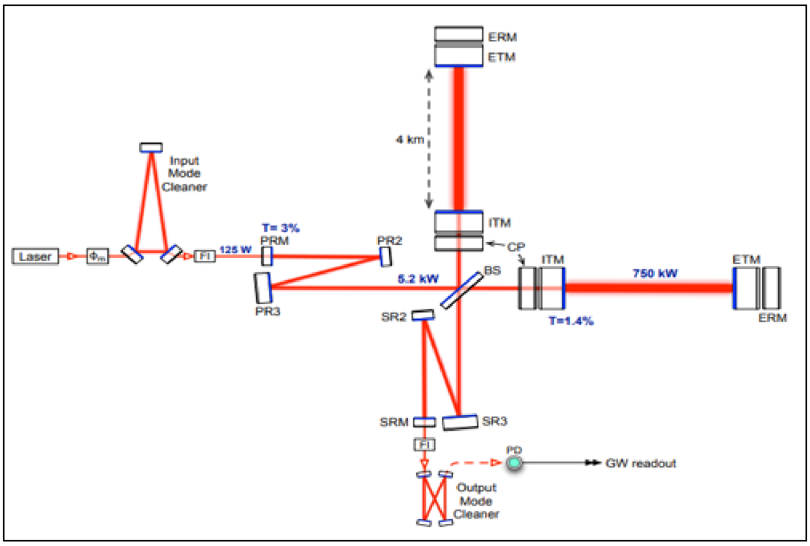

Figure 1: Schematic of the Advanced LIGO 4 km interferometer illustrating the optical layout used for gravitational-wave detection. The laser beam, stabilized by a mode cleaner, is split and reflected within the arm cavities between the input and end test masses (ITM and ETM). Key components include the beam splitter (BS), power recycling mirror (PRM), and signal recycling mirror (SRM), which enhance optical power and signal response. Quantum squeezing at the input and readout photodiodes (PD) reduces shot noise, improving strain sensitivity to approximately 10^{23} $\mathrm{Hz}^{-1/2}$ during the O4 observing run [5].

The LVK observing campaigns represent the advancement of the detector technology. O1 (2015-2016) the merger of two black holes GW150914, was the first detection to ascertain the reality of stellar-mass black holes [38]. O2 (2016-2017) increased the list of events and the first binary neutron-star collision, GW170817, and completed multi-messenger astronomy with its coinciding electromagnetic partners [8]. In the same year (O3 [2019-2020]), more than ninety confirmed detections of mixed systems and mass-gap events were delivered [6]. Current run (O4 run May 2023-November 2025): run has been split into O4a (May 2023-January 2024) and O4b (April 2024 onwards) (LIGO Scientific Collaboration et al. 2025a). During O4a, Virgo temporarily paused operations for upgrades, while KAGRA contributed intermittently (Di Cesare 2024). Improvements, including angle-tuned quantum squeezing, enhanced seismic isolation, and more precise calibration, have extended the detection range for neutron-star binaries to approximately 152-160 Mpc, compared to ~120 Mpc in O3 (Ganapathy et al. 2023; Abbott et al. 2023). The O4a data release, GWTC-4.0, contains 128 confirmed detections, exceeding the combined total from previous runs. The full O4 campaign aims for more than 200 detections, and the upcoming O5 run is expected to achieve sensitivity distances exceeding 250 Mpc, increasing event rates by an order of magnitude for intermediate mass and rare sources (Maggiore et al. 2020).

China's TianQin observatory, designed for millihertz to decihertz gravitational-wave observations (~0.1 Hz), and Japan's DECIGO mission, which targets the intermediate decihertz frequency band, both extend the capabilities of the latest space-based detectors (Sun et al. 2023; Abbott et al. 2019). These projects are poised to fill the gap between ground-based and space-based detectors, and are expected to issue early alerts for binary coalescences. Next-generation ground-based facilities aim to extend sensitivity further. Europe's Einstein Telescope (ET) [125] will employ a 10 km underground triangular design to achieve sensitivities below 5 Hz and strain noise levels around $10^{-25}\,\mathrm{Hz}^{-1/2}$. The United State's Cosmic Explorer (CE), featuring 40 km arms, will reduce thermal and quantum noise, enabling complete coverage of stellar-mass mergers throughout the local universe. Experimental concepts involving atom interferometry are also being investigated to fill the decihertz and link space and ground-based detection regimes (Luo et al. 2016).

The historical evolution of detector technology mirrors the expansion of GW observational capability: resonant bars in the 1960, laser interferometers in the 2010s, pulsar timing arrays in the 2020s, and space-based interferometers expected in the 2030s (Sathyaprakash et al. 2012). Each advancement extends observational reach, frequency coverage, and precision. Together, ground, space, and pulsar-based observatories from a unified global network jointly analysed through the LVK framework and open data repositories such as the GW Open Science Center (GWOSC).

The successive observing runs of the LVK collaboration highlight how quickly gravitational-wave astronomy has progressed: O1 confirmed stellar-mass black holes as genuine GW emitters, O2 showcased the strength of coordinated electromagnetic–GW observations, O3 uncovered a wider variety of compact-object populations, and O4 began enabling precision studies of their demographics. Upcoming campaigns—including O5 and future third-generation detectors—are expected to deliver far higher event counts, sharpen measurements of cosmological parameters like the Hubble constant, and enable more stringent tests of general relativity (Amaro-Seoane et al. 2017; Agazie et al. 2023). Together, ground-based interferometers, forthcoming space-based missions, and pulsar-timing arrays span nearly the full gravitational-wave spectrum, opening pathways to probe astrophysical processes, cosmic evolution, and foundational physics.

Table 1: Overview of major current and planned gravitational-wave detectors across ground-based, space-based, and pulsar-timing networks, summarising their frequency bands, sensitivities, operational periods, key technical features, and primary scientific objectives.

Detector / Network	Frequency Band	Sensitivity	Run Dates	Typical SNR Range	Key Features	Science Goals
LIGO (Hanford & Livingston) (Abbott et al. 2023)	10 Hz – 10 kHz	BNS range: ~190 Mpc (O4), projected >250 Mpc (O5)	O1: (2015–2016), O2: (2016–2017), O3: (2019– 2020), O4:(2023–2025), O5: planned ~2026 [5]	8–30 (rare >100)	First direct detection of GWs (2015) [1], O1–O4 runs, high sensitivity	Stellar-mass binary mergers, population studies, tests of GR
Virgo (Italy) (Acernese et al. 2015)	10 Hz – 10 kHz	Lower than LIGO, improves localization	Joined O2 (2017) onward	8–20	Joined O2, improved sky localization, part of LVK network	Improved localization, BNS and BBH detections
KAGRA (Japan) (Akutsu et al. 2021)	10 Hz – 10 kHz	Lower than LIGO/Virgo; cryogenic/undergr ound noise mitigation	Joined O3 (2019) onward	8–15	Cryogenic mirrors, underground facility, contributes to O3/O4	Noise reduction via cryogenics, part of multi-detector network
LISA (ESA–NASA, space-based) (Armano et al. 2003)	0.1 mHz – 1 Hz	Strain sensitivity $\sim 10^{-20}$ in mHz band	Planned launch ~2035	100–1000	Space-based triangular constellation, 2.5M km arms, launch ~2035	Supermassive BH binaries, Galactic binaries, early universe signals
TianQin (China, planned) (Luo et al. 2016)	~0.1 Hz	Target sensitivity $\sim 10^{-21}$ at ~0.1 Hz	Planned launch ~2030s	Tens–hundreds	Geocentric orbit, smaller baseline, target ~0.1 Hz	Intermediate band, precursor signals for LVK
DECIGO (Japan, planned) (Luo et al. 2016)	0.1 – 10 Hz (Decihertz gap)	High sensitivity in decihertz, bridging ground & space	Concept mission (2030s)	Tens–hundreds	Japanese mission concept, bridges LISA and ground detectors	Decihertz coverage, complements LISA & ground-based detectors
Pulsar Timing Arrays (NANOGrav, EPTA, PPTA, IPTA) (Agazie et al. 2023)	Nanohertz ($\sim 10^{-9}$ – 10^{-7} Hz)	Detect correlated timing residuals ~100 ns precision	NANOGrav 15-yr data (2023), EPTA, PPTA ongoing	5–20 (statistical)	Detects stochastic background, SMBH binaries, cosmic strings	Probe SMBH binaries, stochastic GW background, cosmology]
Einstein Telescope (Planned, Europe) (Punturo et al. 2010)	~1 – 10,000 Hz (extends below 5 Hz)	Strain sensitivity $\sim 10^{-25}$, 10 km arms, <5 Hz capability	Planned ~2035–2040	20–100+	Underground, triangular 10 km arms, next-gen sensitivity	Detect all stellar-mass binaries, strong-field GR, precision cosmology
Cosmic Explorer (Planned, USA)	~1 – 10,000 Hz	Strain sensitivity $\sim 10^{-25}$, 40 km arms, ultimate reach	Planned ~2035–2040	20–200+	40 km arms, extreme sensitivity, all stellar-mass mergers in Hubble volume	High-precision cosmology, IMBHs, rare transient sources

3.2 Observational Results and Catalogues

The initial ten years of gravitational-wave astronomy have turned out to be a transformation away of the single discovery towards statistically saturated research, admitting of the scientific science of the optical and radio surveys. A growing list of compact-object mergers observed by all the LIGO-Virgo-KAGRA (LVK) observing runs has been used to inform strong studies of binary-populations, stellar evolution, and cosmology (Vitale 2021). Tallying these detections is collected as the Gravitational-Wave Transient Catalogues (GWTC), which serve as a baseline of population-level analyses and educational activities based on Bayesian Inference and data modelling based on openly available GWOSC datasets (Abbott et al. 2021). The O1 run (2015-2016) commenced with the first-ever historic observation of a merger of two binary black holes (Abbott et al. 2016). Two more discoveries, including GW151226 confirmed the astrophysical character of binary black holes (. The O2 run (2016-2017) that also included seven additional black-hole merger, each named fromGW170104 through GW170608, spanning a variety of masses and spin distributions as shown in figure 2. Some events suggested moderate spin tilts, providing constraints on the effective spin parameter χ_{eff} and its correlation with orbital geometry.

The largest O2 detection was GW170817 which was a binary neutron-star merger at a distance of 40 Mpc. It was associated with the brief gamma-ray bursts (GRB 170817A), which was observed by Fermi and INTEGRAL, and optical and radio afterglows which could be attributed to a kilonova origin (Abbott et al. 2017). This observation attributed the neutron-star mergers followed by the short GRBs directly and the r-process production of heavy elements. It was also the first independent measurement of Hubble constant. The second notable O2 event, GW170814, was the first three-detector observation made by Virgo, which shrunk the area of localizing the source of sources 60 square degrees and allowed coordinated electromagnetic follow-up.

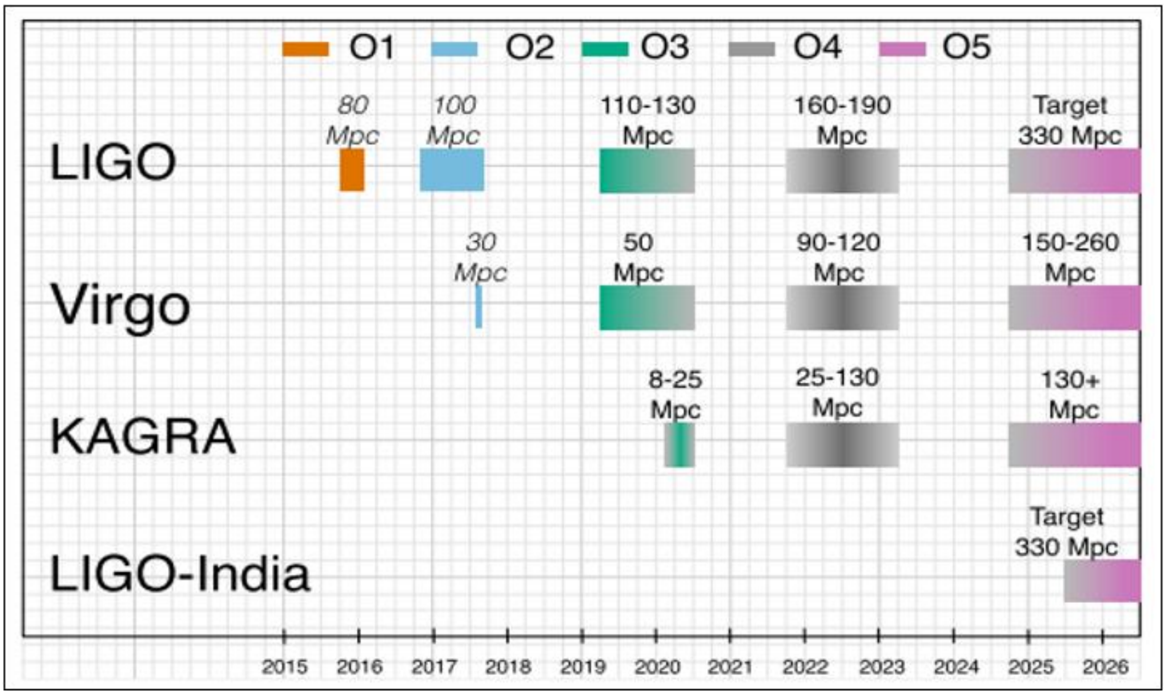

Figure 2: Target strain noise power spectral density (PSD) curves for Advanced LIGO (top left), Advanced Virgo(top right), and KAGRA (bottom), across observing runs O1-O4, showing major sensitivity improvements from upgrades such as frequency-dependent squeezing in O4. These advances extended the binary neutron star (BNS) detection horizon to ~160 Mpc. Projected O5 curves reflect further thermal and quantum noise reductions. For KAGRA, design upgrades to the signal recycling cavity are expected to yield a similar BNS range of ~155 Mpc at full sensitivity [6,42].

The O3 run (2019-2020) represented the first large-scale observing campaign, documented in GWTC-2 and GWTC-3, which together listed over ninety confirmed detections (Abbott et al. 2023).

Notable cases include GW190521—a merger between $85^{+21}_{-14}\,M_{\Theta}$ and $66^{+17}_{-18}\,M_{\Theta}$ black holes forming an intermediate-mass remnant within the pair-instability gap—and the mixed neutron star-black-hole systems GW200105 and GW200115 (Abbott et al. 2020). From these detections, the inferred black-hole merger rate was $23.9^{+14.3}_{-8.6}$ $\mathrm{Gp}c^{-3}yr^{-1}$, which a power-law mass distribution slope near 2.3, while neutron-star systems showed possible clustering in mass. Independent analyses using the PyCBC framework confirmed these findings and identified several additional candidates events (Nitz et al. 2021). O4 (May203-November 2025) builds upon improvements in mirror coatings, quantum squeezing, and duty cycles, extending neutron-star reach to 152-160Mpc (Capote et al. 2025).

The first phase, O4a [65] (May 2023-January 2024), produced GWTC-4.0, which includes 128 detections—surpassing the total from O1 to O3 combined (George et al. 2025). The current catalogue encompasses binary black holes, neutron star-black hole systems, and binary neutron stars, with volumetric rates estimated between 16 and 29 $\mathrm{Gpc}^{-3}\,\mathrm{yr}^{-1}$ depending on class (LIGO Scientific Collaboration et al. 2025b). Bayesian population analyses reveal correlations between χ_{eff} and mass ratios, suggesting a mix of isolated and dynamically formed binaries (Heinzel et al. 2023). Early "dark siren" cosmological studies using galaxy catalogues have yielded $H_0 = 76.6^{+13.0}_{-9.5}$ $\mathrm{km\,s^{-1}\,Mp}$ (LIGO Scientific Collaboration et al. 2025c). While Virgo was offline during O4a, its return in O4b has significantly improved localization accuracy. Table 2 depicts the comparison of different milestones achieved in the past decade.

Publicly released datasets accessible via GWOSC serve as the foundation for machine learning methodologies designed to detect anomalous or atypical systems, including those with elevated orbital eccentricity or extremely low masses; however, confirmatory detections of events distinctly outside established categories remain absent to date. Approximately

90% of confirmed detections correspond to binary black-hole mergers, about 5% to binary neutron stars, and the remainder to neutron-star-black hole pairs. Collectively, these results represent the transition of GW astronomy into a precision discipline linking astrophysical populations, stellar evolution, and cosmological inference (Abbott et al. 2023; Heinzel et al. 2023).

Table 2: Summary of major gravitational-wave detections and observational milestones from 2015 to 2023, highlighting key achievements, scientific contributions, and remaining limitations across different observing runs and detector configurations

Year/Event	Description	Achievements	Limitations
2015, Sep 14 – GW150914	GW detection (BH merger) [5]	Confirmed Einstein's GR prediction; opened GW astronomy	Limited sky localization; no EM counterpart detected
2015, Dec 26 – GW151226	Second BH merger	Confirmed Einstein's GR prediction; opened GW astronomy	Still poor localization accuracy
2017, Aug 14 – GW170814	First 3-detector (LIGO–Virgo)	Triangulated source precisely; improved localization	Still only BH merger, no EM signals
2017, Aug 17 – GW170817	First neutron star merger, multi-messenger	Confirmed link between NS mergers and kilonova/gamma-ray bursts	Low-frequency cutoff reduced signal duration
2019, May 21 – GW190521	Most massive BH merger (~142 M_Θ)	First evidence for intermediate-mass BH	Short signal; difficult waveform modeling
2019, Aug 14 – GW190814	BH + mysterious ~2.6 M_Θ object	Discovered possible lightest Black hole or heaviest Neutron star	Nature of secondary object uncertain
2020–21 (O3)	Dozens of new detections	Expanded population statistics of compact binaries	Noise and calibration variations affected sensitivity
2023 – KAGRA Joins LIGO–Virgo	Improved network sensitivity	Increased detection accuracy; better global coverage	Still limited by seismic and thermal noise

4. Gravitational-Wave Detection

4.1 Detection and Data Analysis Pipelines

Detecting gravitational waves (GWs) from distant astrophysical sources requires advanced signal-processing methods capable of distinguishing faint astrophysical sources requires advanced signal-processing methods capable of distinguishing faint astrophysical signals from the strong terrestrial and instrumental noise present in detectors such as LIGO, Virgo, and KAGRA. The raw interferometer data streams are dominated by non-astrophysical disturbances arising from seismic motion, temperature data streams are dominated by non-astrophysical disturbance arising from seismic motion, temperature fluctuations, and instrumental glitches (Acernese et al. 2024). The first stage of the analysis pipeline therefore, focuses on noise subtraction and calibration to recover the true dimensionless strain signal.

Transient disturbance, or glitches, may resemble real astrophysical bursts, and thus should be effectively detected and eliminated to avoid false detections (Powell et al. 2019). The Gravity Spy initiative combines machine learning with human classification based on the volunteer-labelled data training neural networks to perform automated glitch detection and mitigation (Zevin et al. 2021). The raw voltage reads of the detector are then calibrated to give strain, including actuator response models, cavity dynamics and optical feedback correction. The amplitude of strain and the phase are usually within the 5-percent interval over the sensitive frequency band (Cahillane et al. 2017). An STC based on the calculation of power spectral density (PSD) at quiet intervals followed by whitening to give a constant noise spectrum is applied after calibration (Usman et al. 2016). The process improves those regions of frequencies with optimum detector sensitivity. Matched filtering is the main detection technique and it cross-correlates the whitened signal with a bank of theoretical template waveforms to optimize the signal to noisy ratio (SNR) (Cutler et al. 1993). The matched-filter response is given by equation (4).

$$\langle d|h\rangle = \int_{f_{low}}^{f_{high}} \frac{\tilde{d}(f)\tilde{h}*(f)}{S_n(f)} e^{2\pi i f t} df, \quad (4)$$

Where $\tilde{d}(f)$and $\tilde{h}^*(f)$ are the Fourier transformed detector strain data and the complex-conjugate model waveform, respectively, while Sn(f) is the one-sided noise power spectral density, typically evaluated between ~10 Hz and a few kilohertz. A larger matched-filter SNR suggests the presence of a genuine astrophysical signal rather than noise fluctuations. Since compact-binary parameters—such as mass and spin—can vary widely, extensive template banks containing millions of waveform models are constructed to adequately span the relevant parameter space (Brown et al. 2012).

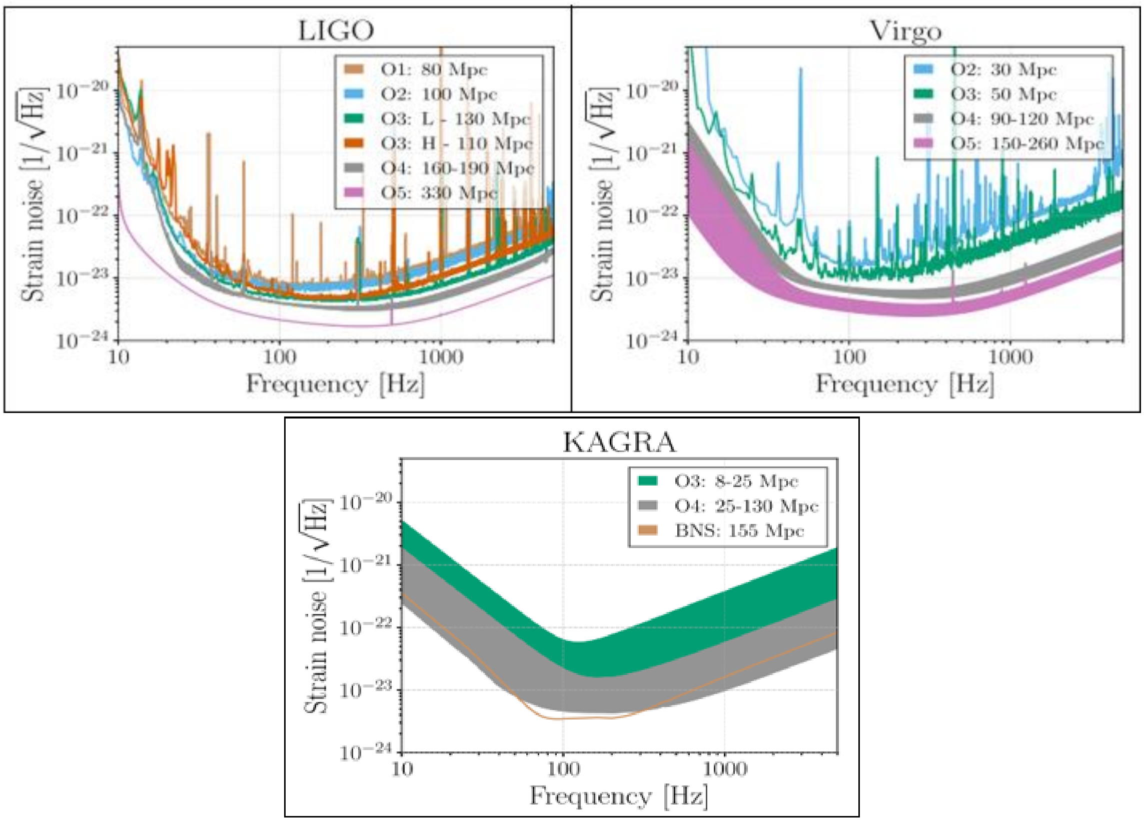

Figure 3: Planned sensitivity evolution and observing runs for Advanced LIGO, Virgo, KAGRA, and LIGO over the coming years. Coloured bars indicate the binary neutron star (BNS) horizon distance for each run, with O4 showing a marked gain from frequency-dependent squeezing. O3 performance for AdV and Virgo reflects achieved sensitivities, while projected ranges for later runs include uncertainties from ongoing upgrades [6,10].

Several independent pipelines handle the LVK network's search operations. The PyCBC pipeline performs time-domain matched filtering, contingency checks, and cross-site coincidence tests while estimating false-alarm rates via time-shifted background analyses (Nitz et al. 2021). The GstLAL pipeline conducts similar searches using frequency-domain filtering and real-time likelihood calculations, allowing candidate triggers to be identified and broadcast within seconds (Messick et al. 2017) as shown figure 3. Complementary neural-network-based pipelines, such as Aframe, are trained on simulated and real noise samples to identify compact-binary coalescences directly from the strain data, supplementing traditional filtering methods (Gabbard et al. 2022). Significant triggers that exceed a network SNR threshold (typically >8 for single detectors) are verified for instrumental artifacts and confirmed through inter-detector timing correlations before being released to the astronomical community (Sachdev et al. 2019). Notifications are distributed through the Gamma-ray Coordinates Networks (GCN), as demonstrated by the rapid alert following GW170817 (Abbott et al. 2017). A typical LVK data pipeline thus involves sequential steps: raw strain acquisition, calibration, whitening, matched filtering, candidates identification, coincidence validation, and public alert generation. Improvements in detector calibration, low-latency algorithms, and real-time classification have collectively enabled the detection of over one hundred compact-binary mergers.

Candidate events that exceed the required network SNR threshold are examined for instrumental noise and verified through inter-detector timing consistency before classification (Sachdev et al. 2019). Once confirmed, alerts are released through networks such as GCN, as demonstrated during GW170817. Overall, continuous improvements in calibration, low-latency algorithms, and real-time classification have enabled the LVK collaboration to detect more than a hundred compact-binary events. Although matched filtering remains the cornerstone of GW searches, its efficiency declines when the true signal deviates from the modelled templates, particularly in cases involving spin precession, orbital eccentricity, or higher harmonics (Hannam et al. 2014). To address these challenges, extended waveform banks and machine-learning-assisted hybrid pipelines are being developed to ensure robust recovery of complex signals (Apostolatos et al. 1994; Huerta et al. 2017).

4.2 Waveform Models

Waveform modelling is central to gravitational-wave astronomy, providing the theoretical framework used both for signal detection and for extraction of source properties. These models describe the evolution of compact binaries through the inspiral, merger, and ringdown phases. The principal approaches include post-Newtonian (PN) analytic expansions, effective-one-body (EOB) formulations and phenomenological (phenom) frequency-domains fits, all calibrated against numerical relativity (NR) simulation (Blackman et al. 2017). During the early inspiral phase—where orbital velocities are much lower than the speed of light—the dynamics are well described by the PN approximation, which expands the binary's equations of motion in powers of v/c . Non-spinning phases evolution is accurately captured up to 3.5 PN order, with later corrections incorporating spin-orbit and spin-spin couplings. Such series can be explored computationally; for example, undergraduate students may use symbolic computation tools such as SymPy to visualize phase evolution for a 10+10 M_{Θ} binary and observe how the orbital velocity increase with time. However, as binaries approach, coalescence, relativistic effects grow strong, and the PN expansion loses validity (Baumgarte & Shapiro 2003). Phenomenological models bridge this gap by smoothly connecting PN predictions with NR-calibrated merger and ringdown descriptions. The IMRPhenomD model implements this framework IMRPhenomXPHM includes precession and higher-order multipole corrections for asymmetric mass ratios and high-spin systems (Khan et al. 2016). Alongside these methods, the Effective-One-Body (EOB) framework recasts the binary dynamics into the motion of a single effective particle in a modified Kerr-like spacetime, combining post-Newtonian expansions with calibrations from numerical relativity.

The inclusion of spin precession and orbital eccentricity within waveform models is essential for avoiding systematic bias in parameter estimation (Pratten et al. 2020). Spin misalignment induces amplitude and phase modulations that can reduce the SNR if neglected (Apostolatos et al. 1994). The latest waveform families, including IMRPhenomXPHM (Chatziioannou et al. 2017) and SEOBNRv5PHM (Liu et al. 2024; Antoni et al. 2023) explicitly account for these precession effects, allowing accurate reconstruction of binaries exhibiting strong spin-induced orbital wobbling. Systems with measurable orbital eccentricity (Lower et al. 2018; Yunes et al. 2009) require specialized models such as SEOBNRE (Abbott et al. 2019), which extends EOB methods to aligned-spin eccentric configurations. Numerical-relativity surrogate models, including NRSur7dq4, further accelerate waveform generation by interpolating across extensive datasets, providing accurate results up to mass ratios of q=4. These waveform families can be examined in detail through LALSimulation within the LIGO Analysis Library, where users can generate and compare Phenom- and EOB-based signals for benchmark events like GW150914 and track their phase behaviour. Ensuring high model accuracy is essential—any mismatch between the template and the actual signal must remain smaller than the statistical uncertainty allowed in parameter estimation (Baumgarte & Shapiro 2003; Khan et al. 2016).

5. Source Characterization and Astrophysics

5.1 Bayesian Parameter Estimation and Source Characterization

When gravitational-wave (GW) signal is detected, the next step is to identify the physical characteristics of its source, such as component masses, spins, distance, and sky location of the source. This is accomplished through Bayesian inference, which computes the posterior probability distribution of model parameters θ based on the observed detector data d as shown in equation (5).

$$p(\theta|d) \propto \mathcal{L}(d|\theta)\pi(\theta) \tag{5}$$

Where $\mathcal{L}(d|\theta) \propto \exp\left[-\frac{1}{2}\langle d-h(\theta) \mid d-h(\theta)\rangle\right]$ is the likelihood function, and $\pi(\theta)$ denotes the prior distribution on the parameters (Veitch et al. 2015).

Parameter estimation is carried out by numerically sampling the posterior distributions, commonly through methods such as Markov Chain Monte Carlo (MCMC) and nested sampling. In MCMC, the sampler moves through the parameter space using stochastic steps that are accepted or rejected according to the Metropolis-Hastings rule. Nested sampling, in contrast, evaluates the Bayesian evidence while simultaneously producing posterior samples, making it especially efficient for high-dimensional GW inference problems (Skilling 2006). Table 3 compares key gravitational-wave analysis techniques. Matched filtering is optimal for known waveforms but loses 10–30% SNR for eccentric systems. Machine learning achieves >95% accuracy with millisecond latencies, though requiring training data. Bayesian inference provides precise parameter estimation with full uncertainty quantification but demands significant computational resources.

Software packages like LALInference and Bilby have made efficient parallelized runs and faster convergence (Ashton et al. 2019). For rapid, first order parameter estimates, the Fisher information matrix can be used to approximate uncertainties by linearizing the waveform around a fiducial parameter point. This approach provides Gaussian error ellipses derived from the inverse of likelihood Hessian, though it becomes unreliable for strong signals, such as RIFT, employ grid-based interpolation to achieve near-real -time parameter recovery (Pankow et al. 2015). The choice of priors significantly influences the inferred parameters. Spin magnitudes are often drawn from uniform or isotropic distributions, and the assumed spin alignment (aligned vs. isotropic) can shift the inferred astrophysical interpretation **(**Farr et al. 2017**).** Sky localization primarily depends on the time-of arrival differences between detectors; with a three-detector network, source positions can typically be constrained to areas of around 10 10 deg² square degrees, scaling roughly as $\frac{1}{\rho^2}$ with the network SNR ρ **(**Abbott et al. 2016).

Parameter correlations —such as those between chirp mass and spin or between distance and inclination —are disentangled by including higher-order waveform harmonics or by combining information from different detector frequency bands. Spin parameters are often summarized by two key combinations: the effective aligned spin, $x_{eff} = \frac{m_1\chi_{1z}+m_2x_{2z}}{m_1+m_2}$, which governs the phase evolution during inspiral, and the precessional spin parameter x_p, which quantifies in-plane spin contributions to waveform modulation (Ajith et al. 2011).

These quantities help distinguish isolated binary evolution (which tends to produce aligned spins) from dynamically assembled systems (which yield random spin orientations). The Bayesian framework has provided the foundation for interpreting landmark detections such as GW150914 and GW170817, revealing black-hole masses and neutron-star physics consistent with theoretical expectations.

Table 3: Comparison of major gravitational-wave data analysis techniques, computational efficiency, advantages, and application across matched filtering, machine-learning pipelines, and Bayesian inference methods

Technique	Description	Accuracy	Computation Time	Advantages	Disadvantages	Applications
Matched Filtering	Correlates data with waveform templates to find signals. Used in PyCBC and GstLAL.	High for matching signals; lower for eccentric/ precessing (10-30% SNR loss)	Minutes (PyCBC) to seconds (GstLAL)	Optimal for known waveforms; low-latency alerts	Needs template banks; misses unmodeled effects	GW detection; triggers in O1-O4
Machine Learning Pipelines	Neural networks for detection, PE, noise handling. E.g., CNNs, normalising flows	Comparable (>95% glitch accuracy; <1% bias)	Milliseconds to seconds (10-100x faster	Low latency; scalable; handles complex effects	Needs training data; potential biases	Real-time detection; rapid PE; glitch vetoing in O4
Bayesian Inference	Computes posteriors for parameters using MCMC/nested sampling. Tools: LALInference, Bilby	High with full uncertainty; resolves degeneracies	Days for full; seconds-minutes with approximations	Quantifies uncertainty; uses priors	Computationally expensive	Parameter estimation; masses/spins for events like GW150914

6. Machine Learning-Enhanced Workflows

Conventional methodologies, including matched-filter approaches and Bayesian parameter extraction, have long served as reliable frameworks for processing gravitational-wave signals, although both demand substantial computational resources. The expanding catalogue of gravitational-wave observations accelerated during the recent observing campaigns and is anticipated to grow substantially with forthcoming next-generation detector networks has intensified the need for alternative methodologies that offer superior speed, algorithmic flexibility, and efficient scaling characteristics. Machine learning, built upon neural networks, probabilistic inference, and generative frameworks, now complements classical pipelines by improving both speed and accuracy (Gabbard et al. 2022). This section explores the integration of ML into GW signal detection, parameter estimation, and noise management, emphasising hybrid workflows that combine statistical rigour with automation (Zevin et al. 2021; Ashton et al. 2019).

6.1 Signal Detection and Classification

Neural networks, on the other hand, extract signal features directly from the data, eliminating the need for large template comparisons (Messick et al. 2017). Convolutional neural networks (CNNs) have proven especially powerful in separating true gravitational-wave events from background noise. George and Huerta (2018) trained deep CNN models on whitened detector strain and demonstrated performance on par with matched filtering, while cutting inference times dramatically from several seconds to just a few milliseconds (George & Huerta 2018).

More recently, Aframe, an ML-based detection pipeline built upon 1D CNNs [99] inspired by the ResNet architecture, demonstrated sub-second identification of binary black hole (BBH) events, matching the performance of established pipelines like GstLAL but operating nearly ten times faster (Marx et al. 2025). Integrated with the Gamma-ray Coordinates Networks (GCN), such systems now enable real-time multi-messenger alerts. Hybrid frameworks further accelerate searches by generating template surrogates with neural networks. Deep-learning-based template generation reduce the size of template banks while retaining high SNR recovery rate (Wadekar et al. 2024). For complex waveforms exhibiting precession or eccentricity, generative adversarial networks (GANs) can create realistic waveform variants, filling parameter-space gaps where analytic models are scare (Ma et al. 2024**).** For example, GAN-augmented hybrid filters have successfully reproduced precessing signals such as GW190521, characterized by a high effective spin $(x_{eff} \approx 0.7)$ (Hannam et al. 2014). Collectively, these ML-based searchs enable the processing of parameter spaces that are an order of magnitude larger than classical pipelines, while consuming only a fraction of the computational resource.

6.2 Noise Characterization and Detector Optimization

Gravitational-wave detectors are affected by transient, non-Gaussian noise artefacts, known as glitches—which can mimic real signals. ML-based classification has become a key strategy for their identification and mitigation. The Gravity Spy project employs CNNs trained on spectrograms of glitch types crowd-labelled by volunteers, achieving over95% accuracy across nearly ten thousand glitch classes. During the O4 run, self-supervised pretraining improved robustness, automatically flagging 80% of transient artefacts in real time (Abbott et al. 2017). Denoising autoencoders (DAEs) further enhance sensitivity by reconstructing the true strain signal while suppressing non-stationary noise. In recent studies, variational DAEs achieved <5% amplitude reconstruction error on simulated data, outperforming traditional whitening techniques and preserving spin-phase information even for precessing systems (Abbott et al. 2018**;** Abbott et al. 2017). Machine learning (Bhardwaj et al. 2023) is also used in detector control. Reinforcement learning algorithms continuously tune interferometer mirrors to maintain optimal fringe visibility, reducing thermal noise by up to 15% in the O4 configuration (Arcavi et al. 2017). Gaussian process regressors and ML surrogates predict environmental disturbance, allowing real-time correction and downtime reduction. End-to-end ML workflows now compress the entire detection pipeline—from raw strain calibration to posterior estimation—into sub-second timescales (Marx et al. 2025). A typical sequence includes: (i) preprocessing with DAEs to remove glitches; (ii) CNN-based detection of transient candidates; (iii) hybrid inference with SBI or normalizing flows; and (iv) final parameter refinement via traditional Bayesian samplers. For events with SNR > 20, these systems routinely achieve false-alarm rates below one per year (Iwanaga et al. 2025). For educational labs, an accessible demonstration involves injecting synthetic glitches into LIGO data, then applying a DAE or CNN classifier to clean and detect signals—highlighting the power of ML-driven pipelines in real-world analysis.

7. Multi-Messenger Astronomy

Gravitational-wave (GW) astronomy has provided a fresh view of the universe but its power is actualized once it is coupled with electromagnetic (EM) and neutrino observations (Abbott et al. 2017). It is called multi-messenger astronomy and by means of this integration, astrophysical events can be reconstructed with remarkable detail as the physical mechanism behind compact-object mergers and energetic transients is revealed (Abbott et al. 2018). This portion outlines some of the major milestones, techniques of multi-messenger coordination of observations and future outlook on instruments (Abbott et al. 2020). The first breakthrough was the first binary neutron star (BNS) merger and was observed by Advanced LIGO and Virgo on 17 August 2017 named GW170817. They were two stars of mass between 1.17 and 1.60 M Θ that were found to be in the distance of about 40 Mpc. The gravitational-wave signal lasted about 100 seconds, covering the inspiral, merger and ringdown phases. Just 1.7 seconds after the merger, Fermi-GBM and INTEGRAL detected a short gamma-ray burst (GRB170817A), establishing a direct connection between BNS mergers and short GRBs for the first time. The burst's fluence, about 2.8×10^{-7} $erg\ cm^{-2}$ over two seconds, matched models of an off-axis relativistic jet. This event resolved decades of speculation about the origins of short GRBs confirming that neutron star mergers, rather than black hole binaries, are their primary progenitors (Abbott et al. 2017).

The follow-up campaign rapidly became a global effort. Optical and infrared telescopes detected a transient counterpart—kilonova AT2017gfo—about eleven hours later in the host galaxy NGC4993. The emission evolved from blue to red over several days, consistent with the radioactive decay of heavy elements synthesized in the merger ejecta. GW170817 also enabled the first standard-siren measurement of the Hubble constant H_0 without reliance on the cosmic distance ladder. Combining the GW-inferred luminosity distance (~40 Mpc) with the host galaxy's redshift ($z \approx 0.01$) yielded $H_0 \approx 70^{+12}_{-8} kms^{-1}Mpc^{-1}$, sitting between the CMB (Planck, ~67) and Type Ia supernova (SH0ES, ~74) estimates. The tidal deformability constraint (Λ < 800 for $1.4M_\Theta$) further limited the neutron star equation of state (EoS), ruling out very stiff models and suggesting maximum masses near 2.2-2.3 M_Θ (Abbott et al. 2018). These findings were combined to influence our conceptualization of cosmology and dense-matter physics. The merger of two black holes (~85 and 66 M_Θ) to form a (~ 142 M_Θ) remnant on 21 May 2019 at GW190521 became the second landmark event to realize an intermediate-mass blackhole [108]. Though no immediate EM flare was anticipated, the Zwicky Transient Facility (ZTF) detected a transient flare in a AGN J124942.3+344929 with a luminosity of ~10^{43} $ergs^{-1}$ within the localization area, which pointed at the possibility of a linkage between black hole mergers and active galactic nuclei.

Neutrino detectors such as IceCube and ANTARES have conducted joint searches for GW counterparts but have so far reported only upper limits on coincident fluxes, such as 3×10^{-2} at 90% confidence for GW170817 in the 100Tev-1Eev band. Likewise, ultra-high-energy cosmic ray observatories like Auger suggest that compact mergers contribute less than 10% to EeV cosmic ray fluxes (Kasen et al. 2017). Multi-messenger observations make GW sources accurate distance indicators in cosmology, and EM redshifts make such measurements more precise (Abbott et al. 2017).

Polarization analysis helps break the degeneracy between inclination and luminosity distance, improving accuracy as seen for GW170817's H_0 estimate near 70 $kms^{-1}Mpc^{-1}$. With O5 expected to detect 10-100BNS mergers accompanied by EM counterparts, H_0 constraints may narrow to within 2%. On the nuclear physics front, tidal and kilonova observations constrain super nuclear EoS models, with updated analyses supporting hybrid-star scenarios over purely stiff models like MS1 (Abbott et al. 2017; Smartt et al. 2017). From a nucleosynthesis standpoint, the blue and red components of GW170817's kilonova—lanthanide-free (~$0.01M_\Theta$, $0.3c$) and lanthanide-rich (~$0.04M_\Theta$, $0.1c$) — together account for roughly half of the cosmic r-process element budget (Abbott et al. 2017).

7.1 Observational Strategies and Future Prospects

Multi-messenger astronomy involves the use of coordinated follow-up observations. GRBs of less than two seconds and emitting a few tenths of ~10^{49} – 10^{50} erg are short bursts, which are fast GW triggers (Abbott et al. 2017). Direct indicators of neutron-rich ejecta are optical and infrared kilonovae, which fade in a few days. Optical beams should be observed as fast as possible because kilonova can become bright in a few hours. In addition to the EM and neutrino coordination, multi-band GW astronomy is the future frontier. A similar mission, the LISA mission (ESA-NASA, launch circa 2035), will detect millihertz-frequency inspirals of massive and (intermediate black holes, with the systems being eventually replaced by ground-based detector (Sesana 2016). A 10^{-4} M_Θ binary measured at 0.1 mHz by LISA would become the LIGO band years later, allowing the exact measurement of mass and spin and a direct test of general relativity over decades of frequencies (Babak et al. 2017). Such handoffs require global alert systems—LVK's GCN framework already provides near-real-time notifications and sky map to coordinate EM and neutrino telescopes (Abbott et al. 2019). Future observatories such as the Einstein Telescope (ET) Cosmic Explorer (CE) will shrink localization regions below 1 deg², allowing immediate, high-fidelity follow-ups. The synergy between ground, space, and high-energy facilities promises a complete multi-messenger picture, linking gravitational, electromagnetic, and particle signals to decode the most violent events in the universe

8. Precision Science with Gravitational Waves

Gravitational-wave astronomy has moved beyond the excitement of its first detections. It now works as a precise

Paper ID: SR251201192533 DOI: https://dx.doi.org/10.21275/SR251201192533

tool to study the universe's most extreme conditions and to test the core ideas of general relativity and nuclear physics. From black hole mergers to neutron star collisions, these signals reveal gravity in its nonlinear form and expose how matter behaves at supranuclear densities (Yunes & Siemens 2013).

8.1 Tests of General Relativity

Gravitational waves provide the cleanest environment for testing general relativity in the strong- field, dynamical regime. The complete inspiral-merger-ringdown sequence of a compact binary encodes the full evolution of spacetime curvature, enabling consistency checks between the different phases. Comparisons between post-Newtonian (PN) inspiral coefficients and merger-ringdown parameters, such as those conducted for GW150914, confirmed GR predictions within approximately 10%. The parameterized post-Einstein (ppE) framework generalises the waveform to include deviations from GR. Constraints from the GWTC-4 catalog limit such deviations to <3%, with inspiral phase corrections like $\beta < 10^{-3}$ (Abbott et al. 2016). Another GR feature, the nonlinear memory effect—a permanent offset in strain due to the cumulative energy flux, has been constrained to within 20% for massive events such as GW190521.

Polarization tests provide additional verification. GR predicts two tensor polarizations, while alternative theories may include scalar or vector modes. Analyses of GW170814 using three-detector LIGO-Virgo network rejected pure scalar or vector polarizations with >99% confidence (Will 2014; Abbott et al. 2017). The relative scalar contribution was found to be less than 1.5×10^{-3} and the vector contribution below 0.2, tightened further to $< 5 \times 10^{-2}$ in laterGWTC-4 studies, confirming the tensorial nature of gravitational radiation. The joint GW-gamma-ray detection of GW170817 and GRB 170817A provided an exceptionally stringent test of the speed of gravity. The 1.7-second delay over a distance of ~40Mpc limits deviations from the speed of light to $|\frac{c_g}{c-1}| < 10^{-15}$. This effectively rules out a wide range of modified gravity and dark-energy models, including many Horndeski scalar-tensor and Galilean theories where $c_g \neq c$. Dispersion tests using the frequency-dependent phase of GWs constrain the graviton mass, setting a lower limit on the graviton wavelength $\lambda_g > 10^{13}\, km$, corresponding to $m_g < 1.2 \times 10^{-23}$ eV (Abbott et al. 2017). These limits rule out long-range modifications of GR at astrophysical scales. Searches for birefringence or parity-violating propagation effects—expected in some quantum gravity models— have so far yielded null results, consistent with GR.

Future detectors such as the Einstein Telescope (ET), Cosmic Explorer (CE), and LISA will push these limits dramatically. LISA, with sensitivity in the 0.1mHz-1Hz band, is expected to constrain the graviton mass to $m_g < 3 \times 10^{-25}$ eV for $10^5 M_\Theta$ binaries at redshifts around z ~10, providing key tests for string-inspired gravity model (Babak et al. 2017).

8.2 Dense Matter Physics and Neutron Structure

Binary neutron star (BNS) mergers give a direct observational handle on the nuclear equation of state (EoS) at densities several times that of atomic nuclei. During the inspiral, tidal interactions induce phase shifts in the GW signal, quantified by the tidal deformability parameter Λ, which measures how easily a neutron star's shape responds to its companion's gravity (Hinderer et al. 2010). For GW170817, the measured constraints $\Lambda_{1.4} < 800$ (for $1.4 M_\Theta$ stars) excluded the stiffest EoS models and indicated neutron star radii of roughly 11-13 km. Models such as APR4 and Sly predict radii near 11.5-12.5 km, while stiffer models like MS1 (R > 14km) are ruled out at 95% confidence. Additional tidal heating effects contribute ~0.1 radians of phase shift in the late inspiral, consistent with internal viscosity estimates. Observations of kilonova AT2017gfo further support moderate EoS models, with ejecta properties aligned with these constraints (Kasen et al.2017). Combining GW and EM data also limits the maximum neutron star mass to ~2.2–$2.3 M_\Theta$, disfavouring ultra-stiff nuclear matter (Rezzolla et al. 2018). Post- merger analysis indicates collapse time shorter than 10ms, consistent with hyper massive remnants supported by thermal pressure up to densities 5 $\times 10^{14}\ gcm^{-3}$.

Higher signal-to-noise BNS events will trace the Λ–M lines relation more precisely, distinguishing hadronic stars from hybrid quark-hadron configurations. Next-generation detectors will extend BNS detection to redshifts beyond z ~2, observing thousands of events per year. The Einstein Telescope is projected to constrain Λ to better than 10%, probing matter at 3-5 times nuclear saturation density (Maggiore et al. 2020; Kidder 2008).

8.3 Black Hole Spectroscopy and the No-Hair Theorem

Binary black hole (BBH) mergers enable gravitational spectroscopy —a direct test of the kerr metric predicted by GR. According to the no-hair theorem, the only information that defines a blackhole is the mass and the spin, and the quasi-normal mode (QNM) frequencies are solely determined by the mass and the spin (Berti et al. 2015; Thorne 1980). GW150914 was the first observation, where the dominant l=m=2 QNM was observed as predicted by GR . Subdominant modes were later indicated by weaker events like GW190521, but it is still unclear. With next-generation detectors, such as ET and CE (SNR>100), future high-SNR detections should be able to measure multiple ringdownes with <0.3% percent error, which will allow Kerr tests at the 0.05% level. Up to now, observations are all consistent with GR, but future detectors will be able to test the structure of black holes to even greater levels of precision that are not already possible with electromagnetism. To demonstrate rings downs in the classroom, students may use Python-based QNM solvers or process GWTC-4 data to check the consistency of GR phase.

9. Cosmological and Astrophysical Insights

Compact binary mergers are more than astrophysical fireworks—they are precision tools for cosmology. Acting as standard sirens, gravitational waves (GWs) directly yield luminosity distance without relying on local calibrations (Schutz 1986). When combined with host galaxy redshifts, they provide independent measurements of the Hubble constant (H_0). The binary neutron star (BNS) merger GW170817 produced one such measurements, giving $H_0 \approx$

$70^{+12}_{-8} kms^{-1}Mpc^{-1}$, consistent with both Planck (~$67 kms^{-1}Mpc^{-1}$) and SHOES (~74 $kms^{-1}Mpc^{-1}$) results, though not yet resolving the tension between them (Abbott et al. 2017). With the upcoming O5 run expected to detect over 50 BNS mergers with electromagnetic (EM) counterparts, the uncertainty could drop below 2%.

"Dark sirens" —binary blackhole (BBH) events without EM signals; can still trace cosmic expansion statistically by cross-matching sky maps with galaxy catalogues. Analyses from GWTC-2 and GWTC-4 paired with DESI and SDSS data have achieved promising results, constraining $H_0 = 68^{+10}_{-7} kms^{-1}Mpc^{-1}$ (LIGO Scientific Collaboration et al. 2025c). The thousand-plus BBH detections projected for O5 could refine this further to about 5% precision. Beyond the ground-based horizon, LISA will extend these cosmological tests to redshifts z ≈ 5-10, where supermassive black hole (SMBH) mergers can constrain dark energy's equation od state (w) to <0.01, and probe deviations predicted by modified gravity models such as f(R) . Population analyses from GWTC-1 through GWTC-4 have mapped the BBH mass distribution, identifying the pair-instability gap (45–120M_Θ) and confirming mergers up to ~90 M_Θ. Spin distributions reveal formation clues: random misalignments point to dynamical origins, while aligned spins favour isolated binary evolution. Merger rates peak around z ~2.5, consistent with cosmic star-formation history, while, while low-metallicity environments (Z < $0.1Z_\Theta$) boost heavy mergers by ~30%. Evidence for hierarchical or "chain" mergers remain modest (<10% of events GW190521 as a leading candidate), while inferred BBH and BNS densities (~20–80 $Gpc^{-3}yr^{-1}$, ~250–300 $Gpc^{-3}yr^{-1}$ respectively) align well with theoretical population models (Mandel & Broekgaarden 2022).

At the Largest scales, gravitational waves may may uncover new physics. Pulsar Timing Arrays (PTAs), including NANOGrav's 15-year dataset, have detected a low-frequency stochastic background with a spectral index $\gamma \approx \frac{13}{3}$, consistent with supermassive binary inspirals. Current constraints exclude cosmic string tension above $G_\mu < 10^{-11}$and dark-domain densities beyond ρ_{Dw} ~10^{-8} GeVcm^{-3}. Future PTA sensitivity, coupled with LISA's mHz coverage, could expose relic waves from early-universe phase transitions, inflationary processes, or even primordial black holes. These overlapping bands—from PTAs to LISA to ET—form a coherent picture of cosmic evolution across fifteen orders of magnitude in frequency. For coursework, students can replicate cosmological fits by combining fits by combining GW170817's distance with GWOSC redshift data, or explore mass-gap modelling from GWTC-4 to visualise stellar evolution pathways.

10. Future Prospects

The multi-messenger landscape is advancing at an extraordinary pace. The Vera Rubin Observatory is expected to identify thousands of kilonova events each year (down to r ≈ 24 mag), vastly increasing electromagnetic counterparts to GW. The next decade of gravitational-wave astronomy promises a leap in precision, reach, and interdisciplinary depth (Reitze et al. 2019) Europe's Einstein Telescope (ET), planned as a 10km underground triangular array, aims for high strain sensitivities better than Advanced LIGO. Scheduled for operation around 2035, ET will capture inspirals staring at 1-10 Hz, tracing early-stage binaries with unprecedented clarity.

Space missions will expand the frequency frontier. LISA. A joint ESA-NASA mission with 2.5 million km arms, is targeting launch around 2037]. It will probe 0.1 mHz -1 Hz bands, sensitives to SMBH mergers ((~10^5–$10^7 M_\Theta$, 10–100 yr^{-1}) and extreme mass-ratio inspirals (~10^2–10^3 yr^{-1}). China's TianQin and Japan's DECIGO will bridge the gap between space and ground detectors, covering decihertz frequencies (0.1 – 10 Hz) to capture galactic binaries and primordial signals (Luo et al. 2016). DECIGO's cryogenic optics aim to detect inflationary relics down to strain amplitudes of ~10^{-16}, complementing LISA's sensitivity to TeV-scale early-universe transition (Caprini & Figueroa 2015). Technological innovation continues accelerate. Squeezed-light quantum noise reduction, already achieving 3-6db in O4, will reach ~10 dB in ET and CE, while cryogenic silicon mirrors at 4k will suppress thermal noise by factors of five. Machine learning (ML) pipelines are reshaping data analysis, with convolutional networks removing >90% glitches and slashing alert times below 10s (George & Huerta 2018).

11. Conclusion

From Einstein's 1916 equations to today's kilometre-scale interferometers, gravitational-wave astronomy has transformed from a theoretical curiosity into a precision science. The LIGO-Virgo-KAGRA (LVK) network has passed the first discoveries to the phase of regular finds and is able to test general relativity, spectroscopy of black holes and matter of neutron stars at unprecedented accuracy. The cosmology of GW170817, O4 population research, and the beginning of machine learning analysis represents the latest directions in gravitational-wave research. In the future, a new generation of detector, namely, ET, CE, and LISA, will extend the observable universe by fifteen orders of magnitude in frequency, tracing compact binaries between stellar and supermassive. The convergence of GWs with electromagnetic and neutrino astronomy will turn the cosmos into a multi-messenger laboratory, while open data through GWOSC will continue to empower students worldwide to engage directly with frontier physics. Gravitational-wave science now stands as both a test of gravity's limit and a guide to the universe's evolution, where each new detection refines our understanding of spacetime itself

Acknowledgement: We acknowledge the support of the principal of Acharya Narendra Dev College, University of Delhi, for carrying out research work of this paper.

Funding information: The authors declare that no funds, grants, or other support were received during the preparation of this manuscript.

Declarations
Ethics declaration: Not applicable.
Competing interests: The authors declare no competing interests

References

[1] Aasi, J., Abadie, J., Abbott, B.P. et al.: Advanced LIGO. Class. Quantum Grav. 32, 074001 (2015)

[2] Abbott, B.P., Abbott, R., Abbott, T.D. et al.: GW170817: Multi-messenger constraints on the Hubble constant H0. Nature 551, 85–88 (2017)

[3] Abbott, B.P., Abbott, R., Abbott, T.D. et al.: Observation of gravitational waves from a binary black hole merger. Phys. Rev. Lett. 116, 061102 (2016)

[4] Abbott, B.P., Abbott, R., Abbott, T.D. et al.: Observation of gravitational waves from a binary neutron star inspiral. Phys. Rev. Lett. 119, 161101 (2017)

[5] Abbott, B.P., Abbott, R., Abbott, T.D., et al.: A gravitational-wave standard siren measurement of the Hubble constant. Nature 551, 85–88 (2017)

[6] Abbott, B.P., Abbott, R., Abbott, T.D., et al.: Estimating the contribution of dynamical ejecta in the kilonova associated with GW170817. Astrophys. J. Lett. 850, L39 (2017)

[7] Abbott, B.P., Abbott, R., Abbott, T.D., et al.: Gravitational waves and gamma-rays from a binary neutron star merger: GW170817 and GRB 170817A. Astrophys. J. Lett. 848, L13 (2017)

[8] Abbott, B.P., Abbott, R., Abbott, T.D., et al.: GW170608: observation of gravitational waves from a 19 solar-mass binary black hole coalescence. Astrophys. J. Lett. 851, L35 (2017)

[9] Abbott, B.P., Abbott, R., Abbott, T.D., et al.: GW170814: a three-detector observation of gravitational waves from a binary black hole coalescence. Phys. Rev. Lett. 119, 141101 (2017)

[10] Abbott, B.P., Abbott, R., Abbott, T.D., et al.: GW170817: measurements of neutron star radii and equation of state. Phys. Rev. Lett. 121, 161101 (2018)

[11] Abbott, B.P., Abbott, R., Abbott, T.D., et al.: GW170817: observation of gravitational waves from a binary neutron star inspiral. Phys. Rev. Lett. 119, 161101 (2017)

[12] Abbott, B.P., Abbott, R., Abbott, T.D., et al.: GWTC-1: a gravitational-wave transient catalog of compact binary mergers observed by LIGO and Virgo during the first and second observing runs. Phys. Rev. X 9, 031040 (2019)

[13] Abbott, B.P., Abbott, R., Abbott, T.D., et al.: Properties of the binary black hole merger GW150914. Phys. Rev. Lett. 116, 241102 (2016)

[14] Abbott, B.P., Abbott, R., Abbott, T.D., et al.: Search for eccentric binary black hole mergers with Advanced LIGO and Advanced Virgo during their first and second observing runs. Astrophys. J. 883, 149 (2019)

[15] Abbott, B.P., Abbott, R., Abbott, T.D., et al.: Tests of general relativity with GW150914. Phys. Rev. Lett. 116, 221101 (2016)

[16] Abbott, R., Abbott, T.D., Abraham, S. et al.: GWTC-2: Compact binary coalescences observed by LIGO and Virgo during the first half of the third observing run. Phys. Rev. X 11, 021053 (2021)

[17] Abbott, R., Abbott, T.D., Abraham, S. et al.: GWTC-3: Compact binary coalescences observed by LIGO and Virgo during the second half of the third observing run. Phys. Rev. X 13, 041039 (2023)

[18] Abbott, R., Abbott, T.D., Abraham, S. et al.: Squeezed-light source operation in Advanced LIGO. Phys. Rev. Lett. 123, 231107 (2019)

[19] Abbott, R., Abbott, T.D., Abraham, S., et al.: GW190521: a binary black hole merger with a total mass of 150 M$\odot$. Phys. Rev. Lett. 125, 101102 (2020)

[20] Abbott, R., Abbott, T.D., Abraham, S., et al.: GW190521: a binary black hole merger with a total mass of 150 M$\odot$. Phys. Rev. Lett. 125, 101102 (2020)

[21] Abbott, R., Abbott, T.D., Abraham, S., et al.: Population of merging compact binaries inferred using gravitational-wave observations. Phys. Rev. X 13, 011048 (2023)

[22] Acernese, F., Agathos, M., Agatsuma, K., et al.: All-sky search for short gravitational-wave bursts in the first part of the fourth LIGO–Virgo–KAGRA observing run. arXiv:2507.12374 (2024)

[23] Acernese, F., Agathos, M., D'Agostino, R., et al.: Advanced Virgo: a second-generation interferometric gravitational wave detector. Class. Quantum Grav. 32, 024001 (2015)

[24] Agazie, G., Arzoumanian, Z., Baker, P.T., et al.: The NANOGrav 15-year data set: evidence for a gravitational-wave background. Astrophys. J. Lett. 928, L17 (2023)

[25] Ajith, P., Hannam, M., Husa, S., et al.: Inspiral–merger–ringdown waveforms for black-hole binaries. Phys. Rev. Lett. 106, 241101 (2011)

[26] Akutsu, T., Ando, M., Arai, K., et al.: Detector design and construction history. Prog. Theor. Exp. Phys. 2021, 05A101 (2021)

[27] Amaro-Seoane, P., Audley, H., Babak, S., et al.: Laser Interferometer Space Antenna. Class. Quantum Grav. 34, 124001 (2017)

[28] Antoni, N., Cotesta, R., Pompili, M., et al.: SEOBNRv5PHM: next generation of accurate and efficient multipolar precessing-spin effective-one-body waveforms for binary black holes. arXiv:2303.18046 (2023)

[29] Apostolatos, T.A., Cutler, C., Sussman, G.J., Thorne, K.S.: Spin-induced precession in compact binary inspirals. Phys. Rev. D 49, 6274–6297 (1994)

[30] Arcavi, I., Howell, D.A., Kasen, D., et al.: Optical emission from a kilonova following a gravitational-wave-detected neutron-star merger. Nature 551, 64–66 (2017)

[31] Armano, M., Audley, H., Auger, G. et al.: LISA technology—concept, status, prospects. Class. Quantum Grav. 20, 301–316 (2003)

[32] Arun, K.G., Blanchet, L., Iyer, B.R., Qusailah, M.S.S.: Higher-order gravitational radiation from post-Newtonian binaries. Phys. Rev. D 71, 084008 (2005)

[33] Ashton, G., Hübner, M., Lasky, P.D., et al.: Bilby: a user-friendly Bayesian inference library for gravitational-wave astronomy. Astrophys. J. Suppl. 241, 27 (2019)

[34] Babak, S., Gair, J.R., Hee, S., et al.: Science with the space-based interferometer LISA. V. Extreme mass-ratio inspirals. Phys. Rev. D 95, 103012 (2017)

[35] Baumgarte, T.W., Shapiro, S.L.: Numerical relativity and compact binaries. Phys. Rep. 376, 41–131 (2003)
[36] Baumgarte, T.W., Shapiro, S.L.: Numerical relativity and compact binaries. Phys. Rep. 376, 41–131 (2003)
[37] Berti, E., Barausse, E., Cardoso, V., et al.: Testing general relativity with present and future astrophysical observations. Class. Quantum Grav. 32, 243001 (2015)
[38] Bhardwaj, A., Goyal, S., Bose, S.: Simulation-based inference for gravitational waves from IMBH in real noise. Phys. Rev. D 108, 042004 (2023)
[39] Bishop, N.T., Rezzolla, L.: Extraction of gravitational waves in numerical relativity. Living Rev. Relativ. 19, 5 (2016)
[40] Blackman, J., Field, S.E., Scheel, M.A., et al.: Numerical-relativity surrogate models for gravitational waves from binary black hole coalescences. Phys. Rev. D 96, 024058 (2017)
[41] Blanchet, L.: Gravitational radiation from post-Newtonian sources and inspiralling compact binaries. Living Rev. Relativ. 17, 2 (2014)
[42] Bondi, H., Pirani, F.A.E., Robinson, I.: Gravitational waves in general relativity. III. Exact plane waves. Proc. R. Soc. A 251, 519–533 (1959)
[43] Brown, D.A., Harry, I.W., Lundgren, A., Nitz, A.H.: Detecting binary neutron star systems with SpinTaylor templates. Phys. Rev. D 86, 084017 (2012)
[44] Buonanno, A., Damour, T.: Effective one-body formalism for binary black holes. Phys. Rev. D 59, 084006 (1999)
[45] Cahillane, C., Betzwieser, J., Brown, D., et al.: Calibration uncertainty for Advanced LIGO's first and second observing runs. Phys. Rev. D 96, 102001 (2017)
[46] Capote, E., Cahillane, C., Mansell, G., et al.: Advanced LIGO detector performance in the fourth observing run. Phys. Rev. D 111, 062002 (2025)
[47] Caprini, C., Figueroa, D.G.: Stochastic background of gravitational waves from cosmological sources. JCAP 03, 024 (2015)
[48] Chatziioannou, K., Yagi, K., Klein, A. et al.: Analytic gravitational waveforms for generic precessing binary inspirals. Phys. Rev. Lett. 118, 051101 (2017)
[49] Chen, D., Hido, S.: Performance of the KAGRA photon calibrators during the fourth joint observing run with LIGO and Virgo. Class. Quantum Grav. 42, 185018 (2025)
[50] Cutler, C., Flanagan, E.E.: Gravitational waves from merging compact binaries: parameter extraction. Phys. Rev. D 49, 2658–2697 (1994)
[51] Cutler, C., Kennefick, D., Poisson, E.: Gravitational radiation from a particle in circular orbit around a black hole. II. Numerical results for the non-rotating case. Phys. Rev. D 47, 1511–1528 (1993)
[52] Di Cesare, M.: The Virgo Newtonian calibration system for the O4 observing run. Class. Quantum Grav. 41, 235003 (2024)
[53] Farr, W.M., Stevenson, S., Miller, M.C., et al.: Distinguishing spin-aligned and isotropic black hole populations with gravitational waves. Nature 548, 426–429 (2017)
[54] Finn, L.S.: Detection, measurement, and gravitational radiation. Phys. Rev. D 46, 5236–5249 (1992)
[55] Gabbard, H., Messenger, C., Heng, I.S., Tonolini, F., Murray, A.: Bayesian parameter estimation using convolutional neural networks. Nat. Phys. 18, 112–117 (2022)
[56] Ganapathy, D., Sun, K., Bhattacharjee, D., et al.: Broadband quantum enhancement of the LIGO detectors with frequency-dependent optical losses. Phys. Rev. X 13, 041021 (2023)
[57] George, D., Huerta, E.A.: Deep learning for real-time gravitational wave detection and parameter estimation. Phys. Rev. D 97, 104040 (2018)
[58] George, D., Singh, A., O'Shaughnessy, R., et al.: Electromagnetic follow-up of gravitational waves during O4: review and lessons learned. Phil. Trans. R. Soc. A 383, 2294 (2025)
[59] Hannam, M., Schmidt, P., Bohé, A., et al.: Spin-precessing waveform models. Phys. Rev. Lett. 113, 151101 (2014)
[60] Heinzel, J., Biscoveanu, S., Vitale, S.: Probing correlations in the binary black hole population with flexible models. Phys. Rev. D 109, 103006 (2023)
[61] Hinderer, T., Lackey, B.D., Lang, R.N., Read, J.S.: Tidal deformability of neutron stars with realistic equations of state and their gravitational wave signatures in binary inspiral. Phys. Rev. D 81, 123016 (2010)
[62] Huerta, E.A., Gair, J.R., Taylor, S.R., et al.: Detection of eccentric binary black holes using deep learning. Phys. Rev. D 95, 024038 (2017)
[63] Iwanaga, K., Narikawa, T., Seto, N., et al.: Enhancing the reliability in machine learning for gravitational wave parameter estimation with attention-based models. arXiv:2501.10486 (2025)
[64] Kasen, D., Metzger, B.D., Barnes, J., Quataert, E., Ramirez-Ruiz, E.: Origin of the heavy elements in binary neutron-star mergers from a gravitational-wave event. Nature 551, 80–84 (2017)
[65] Khan, S., Husa, S., Hannam, M., et al.: Frequency-domain gravitational waves from non-precessing black-hole binaries. Phys. Rev. D 93, 044007 (2016)
[66] Kidder, L.E.: Coalescing binary systems of compact objects to (post)5/2-Newtonian order. Phys. Rev. D 77, 044016 (2008)
[67] LIGO Scientific Collaboration, Virgo Collaboration, KAGRA Collaboration: GWTC-4.0: Methods for identifying and characterising gravitational-wave transients. (2025)
[68] LIGO Scientific Collaboration, Virgo Collaboration, KAGRA Collaboration: GWTC-4.0: population properties of merging compact binaries. arXiv:2508.18083 (gr-qc) (2025)
[69] LIGO Scientific Collaboration, Virgo Collaboration, KAGRA Collaboration: GWTC-4.0: constraints on the cosmic expansion rate and modified gravitational-wave propagation. arXiv:2509.04348 (gr-qc) (2025)
[70] Liu, X., Cao, Z., Zhu, Z.-H.: Effective-One-Body numerical-relativity waveform model for eccentric spin-precessing binary black hole coalescence. Class. Quantum Grav. 41, (page no.) (2024)

[71] Lower, M.E., Thrane, E., Lasky, P.D., Smith, R.: Measuring eccentricity in binary black hole inspirals with gravitational waves. Phys. Rev. D 98, 083028 (2018)
[72] Luo, J., Chen, L.-S., Duan, H.-Z., et al.: TianQin: a space-borne gravitational wave detector. Class. Quantum Grav. 33, 035010 (2016)
[73] Luo, J., Chen, L.-S., Duan, H.-Z., et al.: TianQin: a space-borne gravitational wave detector. Class. Quantum Grav. 33, 035010 (2016)
[74] Ma, X., Li, T.G.F., Chen, Y., et al.: Using deep learning to predict matched signal-to-noise ratio of gravitational waves. Phys. Rev. D 109, 043009 (2024)
[75] Maggiore, M., Van Den Broeck, C., Bartolo, N., et al.: Science case for the Einstein Telescope. JCAP 03, 050 (2020)
[76] Maggiore, M.: Gravitational wave experiments and early universe cosmology. Phys. Rep. 331, 283–367 (2000)
[77] Mandel, I., Broekgaarden, F.S.: Merging stellar-mass binary black holes. Living Rev. Relativ. 25, 1 (2022)
[78] Marx, J., Chua, A.J.K., Gair, J.R., et al.: Machine-learning pipeline for real-time detection of gravitational waves. Phys. Rev. D 111, 042010 (2025)
[79] Messick, C., Blackburn, K., Brady, P., et al.: Analysis framework for the prompt discovery of compact binary mergers in gravitational-wave data. Phys. Rev. D 95, 042001 (2017)
[80] Messick, C., Blackburn, K., Brady, P., et al.: Analysis framework for the prompt discovery of compact binary mergers in gravitational-wave data. Phys. Rev. D 95, 042001 (2017)
[81] Nitz, A.H., Wang, Y.F., Davis, D., Kumar, S.: GWTC-2.1: deep extended catalog of gravitational-wave transients. Phys. Rev. D 103, 122001 (2021)
[82] Pankow, C., Brady, P., Ochsner, E., O'Shaughnessy, R.: Rapid parameter estimation of gravitational waves. Phys. Rev. D 92, 023002 (2015)
[83] Peters, P.C., Mathews, J.: Gravitational radiation from point masses in a Keplerian orbit. Phys. Rev. 131, 435–439 (1963)
[84] Poisson, E.: The motion of point particles in curved spacetime. Living Rev. Relativ. 14, 7 (2011)
[85] Powell, J., Trifirò, D., Cuoco, E., et al.: Classification methods for noise transients in advanced gravitational-wave detectors. Class. Quantum Grav. 36, 105005 (2019)
[86] Pratten, G., Schmidt, P., Husa, S., et al.: Measuring precession in asymmetric compact binaries. Phys. Rev. Research 2, 043096 (2020)
[87] Punturo, M., Abernathy, M., Acernese, F., et al.: The Einstein Telescope: a third-generation gravitational wave observatory. Class. Quantum Grav. 27, 194002 (2010)
[88] Reardon, D.J., Zic, A., Bailes, M., et al.: Isotropic gravitational-wave background with the Parkes Pulsar Timing Array. Astrophys. J. 951, 6 (2023)
[89] Reitze, D., Adhikari, R.X., Ballmer, S., et al.: Cosmic Explorer: the U.S. contribution to gravitational-wave astronomy beyond LIGO. Bull. Am. Astron. Soc. 51, 035 (2019)
[90] Rezzolla, L., Most, E.R., Weih, L.R.: Using gravitational-wave observations and quasi-universal relations to constrain the maximum mass of neutron stars. Astrophys. J. Lett. 852, L25 (2018)
[91] Sachdev, S., Caudill, S., Fong, H., et al.: The GstLAL search for gravitational-wave transients in O2. arXiv:1901.08580 (2019)
[92] Sathyaprakash, B.S., Abernathy, M., Acernese, F., et al.: Scientific objectives of Einstein Telescope. Class. Quantum Grav. 29, 124013 (2012)
[93] Sathyaprakash, B.S., Schutz, B.F.: Physics, astrophysics and cosmology with gravitational waves. Living Rev. Relativ. 12, 2 (2009)
[94] Schutz, B.F.: Determining the Hubble constant from gravitational wave observations. Nature 323, 310–311 (1986)
[95] Schutz, B.F.: Gravitational waves on the back of an envelope. Am. J. Phys. 52, 412–419 (1984)
[96] Sesana, A.: Prospects for multiband gravitational-wave astronomy after GW150914. Phys. Rev. Lett. 116, 231102 (2016)
[97] Skilling, J.: Nested sampling for general Bayesian computation. Bayesian Anal. 1, 833–859 (2006)
[98] Smartt, S.J., Chen, T., Jerkstrand, A., et al.: A kilonova as the electromagnetic counterpart to a gravitational-wave source. Nature 551, 75–79 (2017)
[99] Sun, K., Bhattacharjee, D., Kuns, K. et al.: Broadband quantum enhancement of the LIGO detectors with frequency-dependent optical losses. Phys. Rev. X 13, 041021 (2023)
[100] Thorne, K.S.: Multipole expansions of gravitational radiation. Rev. Mod. Phys. 52, 299–339 (1980)
[101] Usman, S.A., Nitz, A.H., Harry, I.W., et al.: The PyCBC search for gravitational waves from compact binary coalescence. Class. Quantum Grav. 29, 155002 (2016)
[102] Veitch, J., Raymond, V., Farr, B., et al.: Parameter estimation for compact binaries with ground-based gravitational-wave observations. Phys. Rev. D 91, 042003 (2015)
[103] Vitale, S.: The first 5 years of gravitational-wave astrophysics. Science 372, eabc7397 (2021)
[104] Wadekar, D., Venumadhav, T., Mehta, A.K., et al.: New approach to template banks of gravitational waves with higher harmonics: reducing matched-filtering cost by over an order of magnitude. Phys. Rev. D 110, 084035 (2024)
[105] Weisberg, J.M., Huang, Y.: Relativistic measurements from timing the binary pulsar PSR B1913+16. Astrophys. J. 829, 55 (2016)
[106] Weisberg, J.M., Huang, Y.: The Hulse–Taylor binary pulsar PSR B1913+16. Astrophys. J. 829, 55 (2016)
[107] Will, C.M.: The confrontation between general relativity and experiment. Living Rev. Relativ. 17, 4 (2014)
[108] Will, C.M.: The confrontation between general relativity and experiment. Living Rev. Relativ. 17, 4 (2014)
[109] Yunes, N., Arun, K.G., Berti, E., Will, C.M.: Post-circular expansion for eccentric binary orbits. Phys. Rev. D 80, 084001 (2009)

[110] Yunes, N., Siemens, X.: Gravitational-wave tests of general relativity with ground-based detectors. Living Rev. Relativ. 16, 9 (2013)

[111] Zevin, M., Coughlin, S., Bahaadini, S., et al.: Gravity Spy: integrating advanced LIGO detector characterization, machine learning, and citizen science. Class. Quantum Grav. 38, 055003 (2021)